Eur. J. Mineral.
2003, **15**, 185–192

# Santabarbaraite: a new amorphous phosphate mineral

GIOVANNI PRATESI[1], CURZIO CIPRIANI[1], GABRIELE GIULI[2] and WILLIAM D. BIRCH[3]

[1] Museo di Storia Naturale, Sezione di Mineralogia e Litologia, Università di Firenze, Via G. La Pira 4, I-50121 Firenze, Italy; e-mail: gpratesi@geo.unifi.it
[2] Dipartimento di Scienze della Terra, Università di Camerino, Via Gentile III da Varano, I-62032 Camerino, Italy
[3] Museum Victoria, Mineralogy and Petrology Section, Melbourne, Victoria 3001, Australia

**Abstract:** Santabarbaraite is a new amorphous ferric iron hydroxy phosphate hydrate from Valdarno, Tuscany, Italy, the type locality, and Wannon Falls, Victoria, Australia. The mineral is the result of *in situ* oxidation of vivianite, occurring as pseudomorphs after vivianite crystals that are up to 3 mm across in concretionary nodules at the type locality and somewhat larger at Wannon Falls. Santabarbaraite is brown to light-brown in hand specimen, but appears yellowish amber under the microscope and has a similar streak. It is translucent with a distinct vitreous to greasy lustre and is nonfluorescent. It is brittle with a distinct parting along the perfect cleavage of vivianite. The hardness was not measured but the measured density of the type material is 2.42 g/cm$^3$. Optically isotropic, the mineral has a refractive index of 1.695(5). The empirical formula for the type material is $(Fe_{2.64}Mn_{0.13}Mg_{0.07})(PO_4)_2(OH)_{2.45} \cdot 5.1H_2O$, giving a simplified formula of $Fe^{3+}{}_3(PO_4)_2(OH)_3 \cdot 5H_2O$. Santabarbaraite from both localities was analysed by several techniques of X-ray absorption (XANES and EXAFS) and infrared spectroscopy, as well as DTA, DTG and TG. The results show that all the Fe in santabarbaraite is trivalent, associated with the presence of both $H_2O$ and hydroxyl. This is consistent with an oxidation series from vivianite through metavivianite to santabarbaraite, involving progressive oxidation of $Fe^{2+}$ accompanied by conversion of $H_2O$ ligands to OH ions. Such a process leads to a gradual collapse of the vivianite structure as hydrogen bonds are eliminated. Santabarbaraite is the end product of this process and can be thus considered the phosphorus analogue of ferrisymplesite.

**Key-words:** santabarbaraite, new mineral, amorphous, vivianite, *kertschenite.*

## 1. Introduction

Santabarbaraite is a new, amorphous, ferric iron hydroxy phosphate hydrate from Valdarno Superiore (Upper Arno River Valley), Tuscany, Italy. Amorphous substances such as this new mineral are not usually thought to meet the normal requirements for mineral species. Moreover, mineralogists are often reluctant to accept amorphous substances as mineral species, so the term "mineraloid" has sometimes been applied to them. In spite of the previous approval of some amorphous minerals (Rogova *et al.*, 1974; Pollard *et al.*, 1991) by the IMA Commission on New Minerals and Mineral Names (CNMMN), perplexity on amorphous minerals could be, at least partly, shared and great prudence is required in order to confirm the presence of a true chemical compound rather than a mixture.

Nowadays, the difficulty of fully characterizing amorphous substances has been overcome by modern spectroscopic methods which, associated with a chemical analysis, can lead to an unequivocal identification of an amorphous substance. For this reason, the CNMMN criteria for a new mineral species (Nickel & Grice, 1998), clearly state that an amorphous substance can be accepted as a mineral species provided that a set of complete quantitative chemical analyses and physical-chemical data (normally spectroscopic) demonstrates the uniqueness of the phase.

The new mineral species described here, santabarbaraite, has not only been well characterized by appropriate spectroscopic methods (XANES and EXAFS) that reveal the three-dimensional short-range environment of iron and phosphorus atoms in the structure, but it has also been placed in a convincing genetic sequence involving the progressive oxidation of vivianite.

The name is after the mining district where the studied sample was collected. Moreover, it honours the Christian martyr Santa Barbara, the patron saint of miners, who was born in Nicomedia, now Jzmid (Turkey), during the IV$^{th}$ century AD. Both the species and the name were approved (2000-052) by the CNMMN prior to publication. The holotype material (from the Valdarno area) is deposited at the Natural History Museum of the University of Florence, Italy, catalogue No. 2862/RI.

Another occurrence of santabarbaraite, from Wannon Falls, Victoria (Australia), was discovered by one of us

DOI: 10.1127/0935-1221/2003/0015-0185
0935-1221/03/0015-0185 $ 3.60

(W.D.B), making a significant contribution to the final outcome of the approval procedure. Material from Australia is stored in Museum Victoria with catalogue numbers M22892 and M34637.

### 1.1 The name: a choice of clearance

Similar material to santabarbaraite (*i.e.* oxidation products of vivianite not producing X-ray diffraction effects) has been reported in the past (Dormann & Poullen, 1980; Pratesi, 1993) and sometimes referred as to *oxykertschenite*. The terms *kertschenit* and *oxykerchenite* were first used by Popoff (1906) to indicate some iron phosphates from the Kerch Peninsula (German, Kertsch), Crimea. Since then, these terms have been used for several natural products and have also been the subject of a review by Rodgers (1986). As shown in Table 1, the names *kertschenite* and *oxykertschenite* are still used for metavivianite and therefore could not be used for santabarbaraite. Moreover, the material from Victoria contains calcium and shows chemical similarity with a phosphate reported in the literature with the name *eguëite* (see Min. Mag. **16**, 358; Dana 7th II, 955). So, while Rodgers (1986) suggested a re-examination of the triclinic ferri-ferrous hydroxy phosphate hydrate (metavivianite) in order to reinstate the name *kerchenite*, it is clear that *kertschenite* and *oxykertschenite* have never been sufficiently characterized. For sake of completeness, it should be remembered that *bosphorite* has also been used to refer to oxidized vivianite (see Spencer, 1925 and references therein). Therefore, a different name was required to identify the amorphous ferric hydroxy phosphate hydrate.

Table 1. Use of names *kertschenite* and *oxykertschenite* in literature.

| |
|---|
| ***Kertschenit* = oxidized vivianite,** Centralblatt Mineral. Geol. Paläontol. (1906) |
| ***Kerchenite* = oxidized vivianite,** Bull. Acad. Sci. St. Pétersbourg (1907) |
| ***Oxykerchenite* = oxidized *kerchenite*,** Bull. Acad. Sci. St. Pétersbourg (1907) |
| ***Kertschenit* = oxidized vivianite,** Min. Mag. (1907) |
| ***Kertchenit* = oxidized vivianite,** Chem. Abstr. (1907) |
| ***Oxykertschenite* = oxidized vivianite,** Min. Mag. (1910) |
| ***Kertchenite* = oxidized vivianite,** English (1939) |
| ***Oxykertchenite* = oxidized vivianite,** English (1939) |
| ***Oxykerchenite* = oxidized vivianite,** Min. Mag. (1946) |
| ***Kertschenite*-α = oxidized vivianite,** Dana 7th (1951) |
| ***Kertschenite*-β = oxidized vivianite,** Dana 7th (1951) |
| ***Kerchenite*-α, β, γ = oxidized vivianite,** Hey (1962) |
| ***Kertschenite*-γ = oxidized vivianite,** Hey (1962) |
| ***Oxykertschenite* = oxidized vivianite,** Hey (1962) |
| ***Oxykerchenite* = amorphous phosphate,** Bull. Min. (1980) |
| ***Oxykerchenite* = amorphous phosphate,** Bull. Min. (1987) |
| ***Kerchenite* = metavivianite,** Min. Mag.(1986) |
| ***Kertschenite* = oxidized vivianite, metavivianite,** Hey (1993) |
| ***Oxykerchenite* = metavivianite,** Hey (1993) |
| ***Kerchite* = metavivianite(?),** Dana 8th (1997) |
| ***Kertschenite* = metavivianite,** Dana 8th (1997) |
| ***Oxykertschenite* = metavivianite,** Dana 8th (1997) |

## 2. Occurrence

The mineral occurs in clays of the Valdarno Superiore lignite-bearing basin, in the Santa Barbara mining district (Tuscany, Italy), which contains deposits of fluvial and fluvial-lacustrine sediments up to 550 m thick (Lazzarotto & Liotta, 1991). Their age ranges from Upper Pliocene to Middle Pleistocene. The basin substrate consists of Oligocene sandstone towards the south and Miocene sandstone towards the north (Sagri & Magi, 1992). Santabarbaraite can be added to other minerals recorded from this area (Corazza *et al.*, 1994) including two type minerals, grattarolaite and rodolicoite (Cipriani *et al.*, 1997).

Santabarbaraite has been also found in clay underlying Tertiary (Pliocene) basalt, exposed beneath the Wannon Falls about 7 km west of Hamilton, Victoria, Australia. This is a noted locality for excellent specimens of vivianite (Birch & Henry, 1993). In particular, santabarbaraite was detected during examination of some Wannon Falls specimens in the Museum Victoria collections. These specimens had been previously described as vivianite pseudomorphed by limonite, but the limonite was revealed to be santabarbaraite.

## 3. Description and experimental procedure

### 3.1 Appearance, physical and optical properties

In the Valdarno area, santabarbaraite appears as concretionary nodules up to 5–6 cm in diameter that show internal cavities filled by aggregates, up to 2–3 mm across, of sub-millimetric pseudocrystals with the morphology of vivianite. In places, the crystalline aggregates of santabarbaraite show a core of metavivianite. At Wannon Falls, the mineral occurs as pseudomorphs after vivianite crystals, in clusters up to 9 cm across. As santabarbaraite is pseudomorphous after vivianite and metavivianite, the visual aspect of santabarbaraite is crystalline, with sometimes elongated and flattened prismatic habit. The colour is brown or light brown in hand specimen, but yellow-amber under the microscope; the streak is yellow-amber. Santabarbaraite is translucent and displays a vitreous to greasy lustre. No fluorescence appears under UV light. Hardness was not determined. Although mineral is brittle and without distinct cleavage, it shows a good parting following the original perfect cleavage {010} of vivianite. It is neither flexible nor sectile. The measured density, using heavy liquids (by means of LST – solution of sodium heteropolytungstates in water), is 2.42 g/cm$^3$ for the Valdarno material; however, this result could be affected by the presence of submicroscopic fractures within the material. Santabarbaraite is optically isotropic, with an index of refraction, measured using white light, of n = 1.695(5). According to the Gladstone-Dale relationship (Mandarino, 1981), the compatibility index $1-(K_P/K_C)= -0.022$ (Valdarno material) is excellent.

### 3.2 Chemical composition

Material from both localities were examined by optical microscopy and SEM to verify the homogeneity of the sam-

Table 2. Chemical analyses of santabarbaraite from Italy and from Australia.

| | Santabarbaraite (Italy) | | Santabarbaraite (Australia) | | |
|---|---|---|---|---|---|
| Constituent | Wt.% | Range | Wt.% | Range | Probe Standard |
| $Fe_2O_3$ | 43.97 | ±0.35 | 43.22 | ±0.35 | Ilmenite – Vivianite |
| $P_2O_5$ | 29.48 | ±0.25 | 28.60 | ±0.25 | Apatite – Vivianite |
| $Mn_2O_3$ | 2.23 | ±0.10 | - - | | Bustamite |
| CaO | - - | | 2.93 | ±0.10 | Diopside |
| MgO | 0.61 | ±0.05 | 0.69 | ±0.05 | Olivine |
| $H_2O$ | 23.90 | ±0.50 | 23.05 | ±0.20 | |
| Total | 100.19 | | 98.49 | | |

ples. Chemical compositions were obtained using a JEOL JXA 8600 electron microprobe equipped with a wavelength-dispersive system. The operating conditions were 15 kV and a beam current of 10 nA, with the beam defocused to 25 microns in order to minimise water loss and prevent damage on the sample surface. Thirty analyses were carried out on three distinct granules of the Valdarno material, and twelve analyses were performed on the Wannon Falls material. The water content was measured by three different analytical methods, namely infrared spectroscopy, thermogravimetry and loss on ignition. Two different methods were used to test for the presence of ferrous iron: titration with standard dichromate solution and X-ray absorption spectroscopy. As shown in Table 2, the analyses and chemical formulae for the mineral from the two localities show only slight differences. In particular, the analytical total is lower for the Australian material, probably due to a different water content, and the Italian sample contains about 2 % Mn, whereas the Australian sample contains about 3 % Ca. Thus, the empirical formulae, based on 2 $PO_4$ anionic groups, can be written as follows: $(Fe_{2.64}Mn_{0.13}Mg_{0.07})(PO_4)_2(OH)_{2.45}\cdot 5.1H_2O$ for santabarbaraite from Valdarno and $(Fe_{2.69}Ca_{0.26}Mg_{0.08})(PO_4)_2(OH)_{2.75}\cdot 5.0H_2O$ for santabarbaraite from Wannon Falls. The simplified formula for both is $Fe^{3+}{}_3(PO_4)_2(OH)_3\cdot 5H_2O$.

### 3.3 X-ray absorption spectroscopy (XANES and EXAFS)

#### *3.3.1 Experimental settings*

Fe K-edge spectra were collected at the GILDA beamline of the ESRF storage ring (Grenoble, F), operating at 6 GeV and with ring currents ranging from 50 to 90 mA. Radiation was monochromatized by means of two Si (3 1 1) crystals, and higher harmonic rejection was achieved by detuning the second crystal. The samples were prepared as finely ground powder deposited onto a kapton tape. The fluorescence yield was measured by a 13-element high purity Ge detector, and the incident intensity by an ionisation chamber. The spectra were collected in step-scan mode ranging in energy from 7000 to 7700 eV with an energy step of 0.2 eV in the edge region and increasing up to 3.0 eV in the high-energy part of the spectrum. Experimental resolution in this energy region is close to 0.2 eV. Taking into account both the geometrical resolution and intrinsic line-width at the Fe K-edge, the width of the spectral features amounts to about 1.1 eV in the edge region. The energy positions are reproducible to ± 0.1 eV. Energy was calibrated against an Fe-Foil (7112 eV).

P K-edge spectra were collected at the B03-3 beamline of the SSRL storage ring (Stanford, CA, USA) operating at 3 Gev and with ring currents ranging from 60 to 90 mA. Radiation was monochromatized by means ot two Ge (1 1 1) crystals, and higher harmonic rejection was achieved by detuning the second crystal. The samples were prepared by allowing the finely ground powder to settle in acetone on a Ag-coated sample-holder. The total electron yield and the incident radiation intensity were measured by two channelthrons positioned, respectively, near the sample and a metallic net halfway between the monochromator and the sample chamber. Further details on the experimental set-up can be found in Wong *et al.* (1994). The spectra were collected in step-scan mode ranging in energy from 2100 to 2120 eV with an energy step of 0.5 eV. Energy resolution amounted to about 0.5 eV, and the reproducibility of the energy position of the XANES features is ± 0.25 eV.

The XANES spectra were reduced by subtracting a linear background and by normalizing the step height to unity, taking it as the mean value of the absorption coefficient in the range 50–100 eV above the absorption edge. Energy was calibrated against a standard of Fe metal (7112 eV). The threshold energy was taken as the first maximum of the first derivative of the spectra, whereas peak positions were obtained by calculating the second derivative of the spectra. Pre-edge peak analysis was carried out following the same procedure reported in Wilke *et al.* (2001). The pre-edge peak was fitted by a sum of pseudo-Voigt function, and the integrated intensities along with centroid energies were compared with those of the standards analysed here and others from the literature (Wilke *et al.*, 2001; Farges, 2001; Giuli *et al.*, 2003)[1] in order to extract information on Fe oxidation state and coordination number in the amorphous phase studied. The EXAFS spectra were analysed by means of the GNXAS code (Filipponi & Di Cicco, 2000). The amplitude factor ($S_0^2$) was kept near 0.83 in fair agreement with the values reported in Farges *et al.* (1994) and Di Cicco *et al.* (1994). Further details on the fitting procedure of the EXAFS spectra can be found in Giuli *et al.* (2003).

#### *3.3.2 Fe XANES of vivianite and santabarbaraite*

The Fe XANES spectra of vivianite and santabarbaraite, both collected at the same locality (Santa Barbara), are shown together in Fig. 1 for direct comparison. Each peak is labeled with a letter, and the spectral features (edge energy, peak positions) are reported in Table 3. The shift of the santabarbaraite spectrum towards higher energy is evident and

[1] The data of Wilke *et al.* (2001) and Farges (2001) are calibrated imposing the metal Fe K-edge at 7112.92 eV. In order to be compared with our data (calibrated at 7112.92 eV), the data of Wilke *et al.* (2001) and Farges (2001) are re-scaled accordingly.

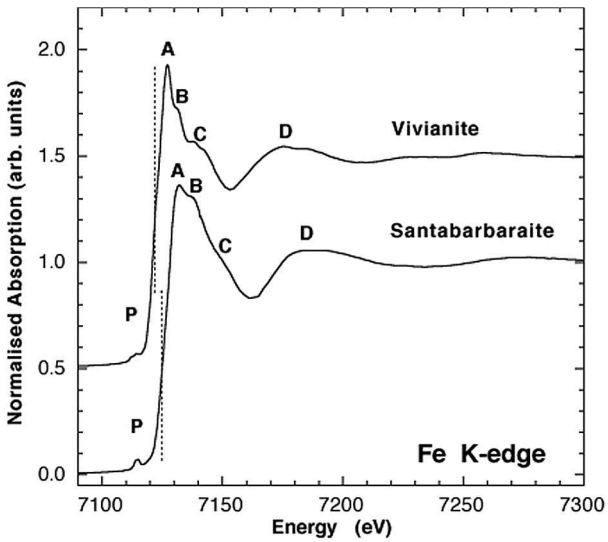


Fig. 1. Fe XANES: absorption spectra of vivianite and santabarbaraite.

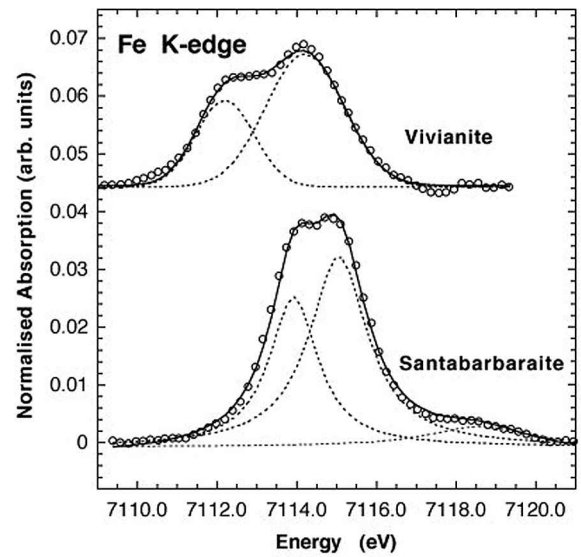


Fig. 2. Fe XANES: pre-edge peaks of the vivianite and santabarbaraite spectra.

Table 3. Peak positions of the Fe K-edge XANES spectra.

| Sample | P[a] | $E_0$[b] | A[a] | B[a] | C[a] | D[a] |
|---|---|---|---|---|---|---|
| Vivianite | 7112.0 | 7120.8 | 7127.2 | 7131.7 | 7138.0 | 7173 |
| | 7114.2 | | | | 7142.6 | 7188 |
| Santabar- | 7113.8 | 7124.5 | 7130.2 | 7137.9 | 7149.2 | 7178 |
| baraite | 7115.1 | | | | | 7194 |

[a] Deduced from the minima in the second derivative spectra.
[b] Deduced from the maximum in the first derivative spectra.

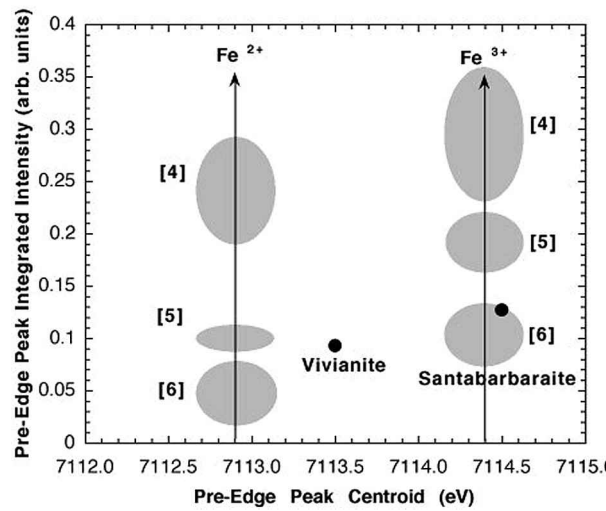


Fig. 3. Integrated intensity and centroid energy position of the Fe XANES pre-edge peaks of vivianite and santabarbaraite.

results from iron oxidation. Comparison of the edge energy of the santabarbaraite spectrum with those of standard compounds suggests that Fe is in the trivalent oxidation state.

The information obtainable from an accurate analysis of the pre-edge peak is more detailed than that derived from the absorption edge alone. This is because it is possible to discriminate the contributions from different Fe oxidation states and thus determine Fe oxidation state as well as coordination number (Waychunas *et al.*, 1983; Calas & Petiau, 1983; Calas *et al.*, 1984; Wilke *et al.*, 2001 and references therein). The pre-edge peaks of the vivianite and santabarbaraite spectra are shown in Fig. 2, along with the contributions into which the peaks are deconvoluted. The integrated intensity and the centroid energy of these spectra are reported in Fig. 3, along with the fields found for Fe standards of known oxidation state and coordination number reported in this study and in Wilke *et al.* (2001). The integrated intensity and centroid energy position of the pre-edge peak of the santabarbaraite spectrum is consistent with trivalent Fe in six-fold coordination. In contrast, the results for vivianite are consistent with a phase showing an ongoing oxidation of iron to yield a mixture of divalent and trivalent Fe in six-fold coordination. Such rapid oxidation is typical of vivianite, so it can be assumed that all vivianites contain a variable percentage of trivalent iron and the chemical formula showing all of the iron as divalent is only a theoretical formula.

### *3.3.3 Fe K-edge EXAFS spectrum of santabarbaraite*

Fig. 4 shows the experimental, theoretical and residual $K^2$ weighted $\chi(K)$ signals (upper panel) along with their Fourier Transforms (lower panel). The experimental signal is well reproduced by the theoretical one up to a wave vector K=12 $Å^{-1}$. In addition, the Fourier Transforms of the two signals are in good agreement. Several trials were performed to fit the experimental spectrum by assuming a regular geometry around iron (tetrahedron, trigonal dipyramid, or octahedron), but none of them was satisfactory. Refining the coordination number only yielded good results with a coordination number equal to 6.0; thus, the experimental spectrum was fitted with theoretical signals calculated assuming a distorted octahedral environment around iron. Several strategies were employed, using a two-shell model (two sets of

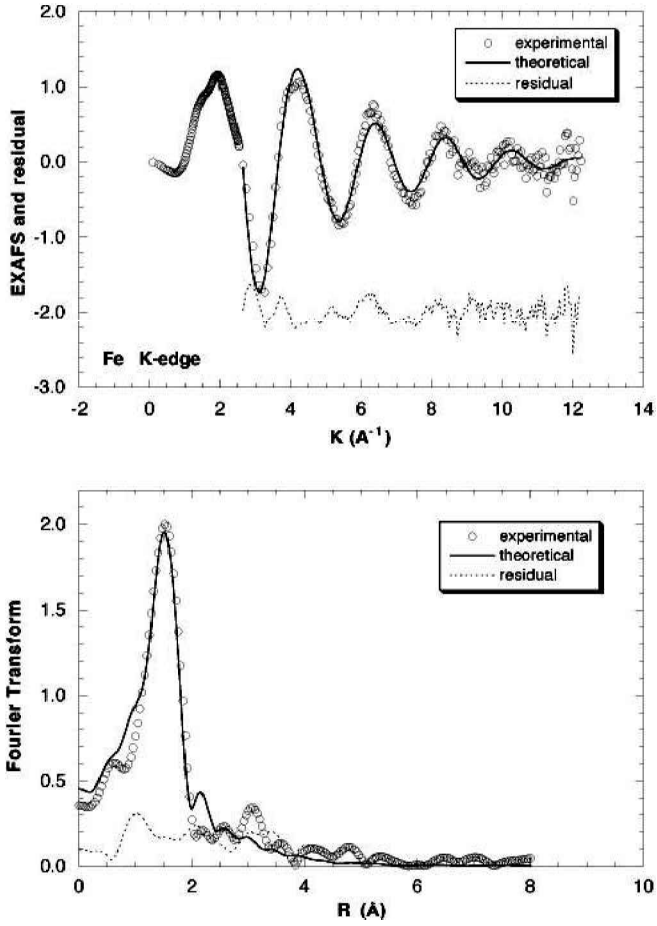


Fig. 4. Fe K-edge EXAFS spectrum of santabarbaraite: experimental, theoretical and residual $K^2$ weighted $\chi(K)$ signals (upper panel) and their Fourier Transform (lower panel).

distances, one short and one long) and a three-shell model (three sets of distances). Both models resulted in good agreement between experimental and theoretical signals, so that at present it is not possible to evaluate the exact Fe-O distance distribution in the amorphous phase. However, the mean <Fe-O> distance obtained using different models always clusters near 2.045 Å ± 0.02. Table 4 shows the best fit obtained by considering three different distances.

### *3.3.4 P K-edge XANES of vivianite and santabarbaraite*

The P K-edge XANES spectra of vivianite and santabarbaraite are shown in Fig. 5. It can be easily seen that the santabarbaraite spectrum is shifted to higher energy in comparison to vivianite. Moreover, the intensity of the white line is clearly lower in the santabarbaraite spectrum. In the absence of a precise energy calibration, no quantitative information can be obtained from these P K-edge spectra. Moreover, since there is no evidence that the topology of the structure maintains unaltered during the transformation to santabarbaraite, no indications can be obtained from Natoli's rule as regards the P-O distances. However, the energy shift observed for the white line is consistent with a change in the P second-coordination shell: *i.e.* corresponding to the oxidation of Fe from divalent to trivalent. According to Franke & Hormes (1995), there is a negative relation between the energy of the white line and its intensity: thus, both variations observed in the experimental spectra are compatible with a change in the oxidation state of the cations in the second coordination sphere of P (in our case Fe) from 2+ to 3+.

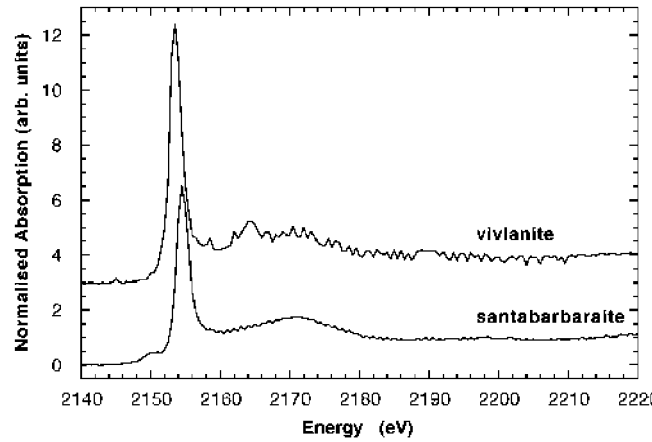


Fig. 5. P K-edge XANES spectra of vivianite and santabarbaraite.

### 3.4 Infrared spectroscopy

Reflectance FTIR spectra of small (mm size) polished grains of the mineral were collected on a Perkin-Elmer Spectrum 2000 Fourier-transform infrared spectrometer using a liquid nitrogen cooled HgCdTe (MCT) detector. The spectra were taken, at a resolution of 4 $cm^{-1}$, in the wavenumber range 5000–700 $cm^{-1}$; the number of scans was 32 for each spectrum.

In the 1300–5000 $cm^{-1}$ region of the FTIR spectra of santabarbaraite from Valdarno (Fig. 6), one main band and three minor bands can be observed. The first, at 3570 $cm^{-1}$, is quite broad and strong, whereas the others at 4455, 1675 and 1475 $cm^{-1}$ are weak. The band at 3570 $cm^{-1}$ also appears in vivianite and represents the main vibrational modes related to the water molecules. Following the suggestion of Piriou & Poullen (1987), this band, which in vivianite is composed of three bands at 3485 $cm^{-1}$ ($\nu'_3(W_{II})$), 3140 $cm^{-1}$ ($\nu_3(W_I)$) and 3280 $cm^{-1}$ ($\nu'_1(W_{II})$), changes progressively in shape and energy as alteration proceeds. Such a change can be ascribed to the appearance of hydroxyl groups that form at the expense of water molecules. The bands at 4455 and 1675 $cm^{-1}$ can be related, respectively, to the $\nu_2+\nu_3(W_I)$ and $\nu_2$ mode of deformation of $H_2O$. Finally, the bands at 2360 and 2341 $cm^{-1}$, that are visible in both the spectra, are due

Table 4. EXAFS refined structural parameters.

| contribution | multiplicity | R (Å) | σ (Å$^2$) |
|---|---|---|---|
| Fe-O | 3 | 1.98 (0.02) | 0.005 |
| Fe-O | 2 | 2.00 (0.02) | 0.019 |
| Fe-O | 1 | 2.29 (0.02) | 0.011 |
| <Fe-O> | 6.0 (0.4) | 2.04 (0.02) | |

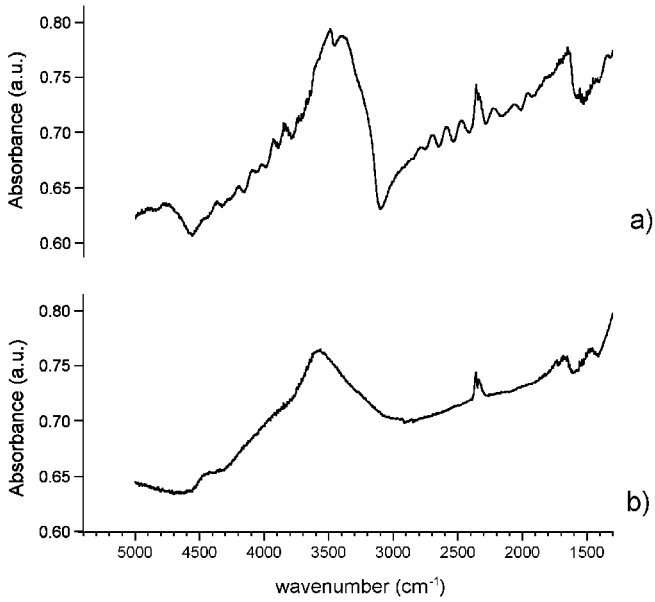


Fig. 6. FTIR spectra of vivianite (a) and santabarbaraite (b) from Valdarno (Italy), in the range 1300–5000 $cm^{-1}$.

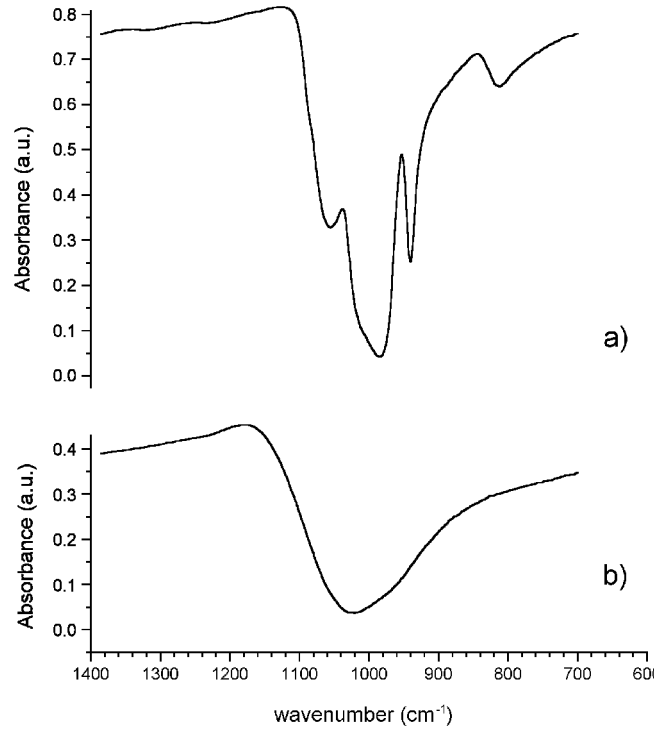


Fig. 7. P-O stretching vibrations of vivianite (a) and santabarbaraite (b), in the range 900–1100 $cm^{-1}$.

to the absorption of $CO_2$ molecules, because the measurements were performed in air.

For the $PO_4^{3-}$ group, it should be borne in mind that the free ion has $T_d$ symmetry, giving rise to four normal modes of vibration, namely $A_1$, ($\nu_1$), E ($\nu_2$), and 2 x $T_2$ ($\nu_3$ and $\nu_4$). The P–O stretching vibrations are clearly visible in the range 900–1100 $cm^{-1}$. In the spectra shown in Fig. 7, the differences between santabarbaraite and vivianite are reported: the santabarbaraite band is simple and unique, whereas the vivianite bands are multiple. It is noteworthy that the shift in the main absorption band of santabarbaraite, from 1125 $cm^{-1}$ of vivianite to 1180 $cm^{-1}$, probably reflects a slight variation in the P–O bond strength.

### 3.5 Thermal data

Thermal analyses were performed on the santabarbaraite from Valdarno as well as from Wannon Falls. Fig. 8 shows DTA, DTG and TG data obtained with a heating rate of 3°C/min. The differential thermal analysis (DTA) shows a broad endothermic peak, spanning 100–250°C, due to loss of water. Santabarbaraite does not show the exothermic peak visible in vivianite at 130°C (due to the oxidation of $Fe^{2+}$) because here the iron is already oxidized to $Fe^{3+}$. The strong exothermic peak at about 650°C represents the recrystallization of two ferric iron anhydrous phosphates corresponding to the minerals grattarolaite and rodolicoite. Thermal gravimetry (TG) and differential thermal gravimetry (DTG) analyses show evidence for both water molecules and hydroxide groups, which are lost in the ranges 100–250°C and 300–450°C, respectively.

For the Wannon Falls material, thermal data confirm both the $H_2O$ and $OH^-$ contents. The spectra strongly resemble those of the Valdarno santabarbaraite. In particular, TG analyses on the Australian occurrence, where more material was available, allowed confirmation of the relative percentage of $H_2O$ and $OH^-$. It is worth mentioning that the $OH^-$ content necessary for charge balance is the actual amount of $OH^-$ calculated from thermogravimetry, where the two distinct effects (one for $H_2O$ and the other for $OH^-$) are clearly visible.

## 4. Discussion and conclusions

As stated by the CNMMN (Nickel & Grice, 1998), a naturally occurring amorphous phase can be accepted as a new mineral provided that complete quantitative chemical analyses and spectroscopic data are available to demonstrate the uniqueness of the phase. Nickel (1995) stated that "noncrystalline substances can be divided into two categories: (1) amorphous substances that have never been crystalline and do not diffract X-rays or electrons and (2) metamict, those that were crystalline at one time, but whose crystallinity has been destroyed by ionizing radiation". Santabarbaraite has never been crystalline as $Fe^{3+}{}_3(PO_4)_2(OH)_3{\cdot}5H_2O$, but it previously existed in a crystalline form as vivianite $Fe^{2+}{}_3(PO_4)_2{\cdot}8H_2O$ (monoclinic) and metavivianite $Fe^{2+}{}_{3-x}Fe^{3+}{}_x(PO_4)_2(OH)_x{\cdot}(8–x)H_2O$ (triclinic).

The oxidation of vivianite to metavivianite is a well-known process investigated with several methods and described by many authors (Dormann & Poullen, 1980; McCammon & Burns, 1980; Dormann *et al.*, 1982). The crystal structure of vivianite contains $Fe^{2+}$ ions in isolated $Fe_A{}^{2+}$ octahedra and in paired $Fe_B{}^{2+}$ octahedra. Spectral

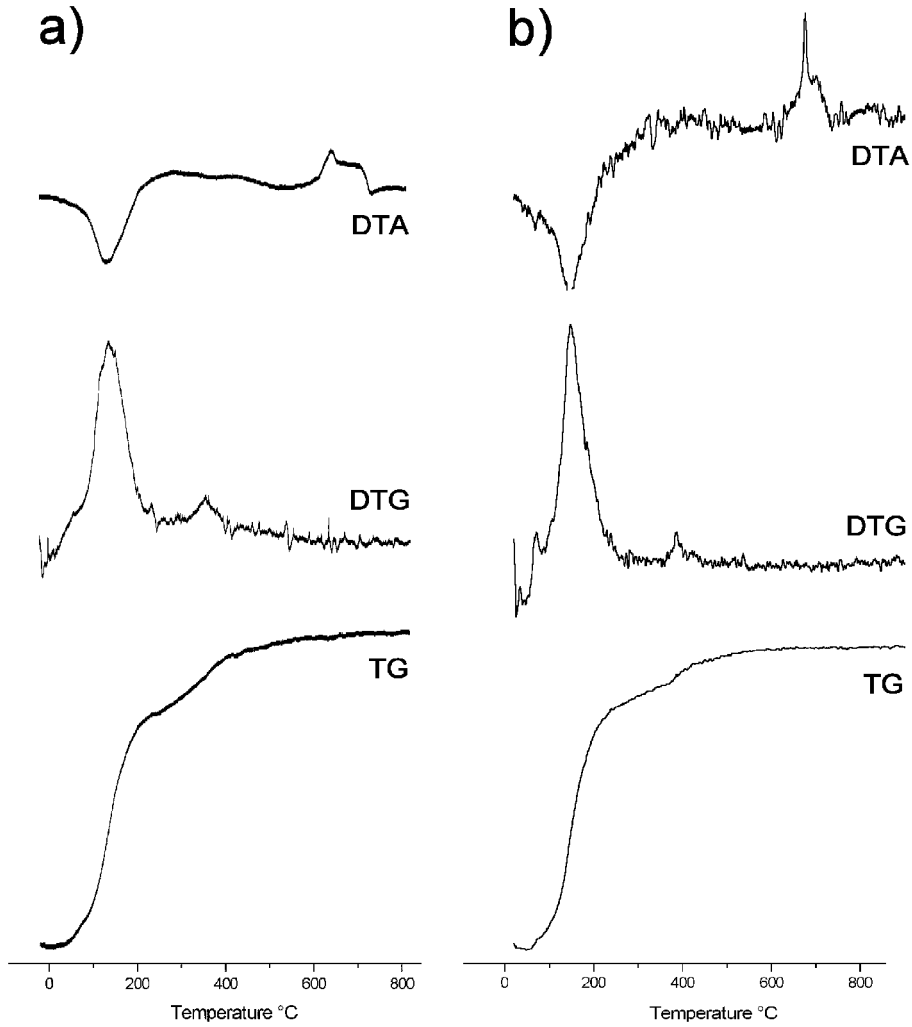


Fig. 8. Thermal analysis of santabarbaraite: a) sample from Valdarno (Italy); b) sample from Wannon Falls (Australia).

measurements (McCammon & Burns, 1980) demonstrated that $Fe_B^{2+}/Fe_A^{2+}$ increases with rising $Fe^{3+}$ concentration, suggesting that the remaining $Fe_A^{2+}$ ions can be more easily oxidized than the second $Fe_B^{2+}$ ion of an $Fe_B^{2+}$-$Fe_B^{3+}$ pair. The mechanism of oxidation of $Fe^{2+}$ ions involves $H_2O$ ligands, which are converted to $OH^-$ ions, producing a progressive collapse of the vivianite structure due to the elimination of hydrogen bonds (Moore, 1971). Dormann & Poullen (1980) stressed that the monoclinic structure of vivianite is maintained until 40 % of the total iron is oxidized. Further oxidation leads to the formation of the triclinic phase metavivianite, in which the $Fe_A$ site is completely oxidized, whereas the oxidation of the $Fe_B$ ranges from 20 % up to almost 100 %. When all of the iron is oxidized, santabarbaraite can then form. In spite of the amorphous state of this phase, the genetic relationship between santabarbaraite and vivianite is straightforward. Moreover, its chemical composition is narrowly confined, since santabarbaraite is the oxidized amorphous ferric end-member arising from the alteration of vivianite. Thus, the full sequence can be shown as follows: monoclinic vivianite → triclinic metavivianite → amorphous santabarbaraite → recrystallization to grattarolaite and rodolicoite.

**Acknowledgements:** The authors are grateful to Mirko Bonechi and Lido Boanini for providing the samples and for some collaborative field campaigns. Thanks are also due to Dr. Andrea Tombesi (C.I.G.S. – University of Modena) for his help in IR analyses, and to the staff of BM-08 (ESRF) and B03-3 (SSRL) for their help during the data collection. Moreover, we acknowledge two anonymous referees for useful suggestions. This research has been supported by the financial support of the Consiglio Nazionale delle Ricerche, Italy.

## References

Birch, W.D. & Henry, D.A. (1993): Phosphate Minerals of Victoria. The Mineralogical Society of Victoria, Spec. Publ. No. 3. Victoria, 184 p.

Calas, G. & Petiau, J. (1983): Coordination of iron in oxide glasses

through high-resolution K-edge spectra: information from the pre-edge. *Solid State Comm.*, **48**, 625-629.

Calas, G., Basset, W.A., Petiau, J., Steinberg, M., Thcoubar, D., Zarka, A. (1984): Some mineralogical application of synchrotron radiation. *Phys. Chem. Minerals*, **11**, 17-36.

Cipriani, C., Mellini, M., Pratesi, G., Viti, C. (1997): Rodolicoite and grattarolaite, two new phosphate minerals from Santa Barbara Mine, Italy. *Eur. J. Mineral.*, **9**, 1101-1106.

Corazza, M., Pratesi, G., Braga, R. (1994): Minerals of the Upper Arno River Valley (Tuscany, Italy). *Mineral. Rec.*, **25**, 293-299.

Di Cicco, A., Berrettoni, M., Stizza, S., Bonetti, E., Cocco, G. (1994): Microstructural defects in nanocrystaline iron probed by X-ray Absorption Spectroscopy. *Phys. Rev.*, ***B*50**(17), 12386-12397.

Dormann, J.L. & Poullen, J.F. (1980): Étude par spectroscopie Mössbauer de vivianites oxydées naturelles. *Bull. Minéral.*, **103**, 633-639.

Dormann, J.L., Gaspérin, M., Poullen, J.F. (1982): Étude structurale de la séquence d'oxydation de la vivianite $Fe_3(PO_4)_2 \cdot 8H_2O$. *Bull. Minéral.*, **105**, 147-160.

Farges, F. (2001): Crystal-chemistry of Fe in natural grandidierites: a XAFS spectroscopy study at the Fe K-edge. *Phys. Chem. Minerals*, **28**, 619-629.

Farges, F., Guyot, F. Andrault, D., Wang, Y. (1994): Local structure around Fe in $Mg_{0.9}Fe_{0.1}SiO_3$ perovskite: an X-ray absorption spectroscopic study at the Fe K-edge. *Eur. J. Mineral.*, **6**, 303-312.

Filipponi, A. & Di Cicco, A. (2000): GNXAS: a software package for advanced EXAFS multiple-scattering calculations and data-analysis. *Task Quart.*, **4**, 575-669.

Franke, R. & Hormes, J. (1995): The P K-near edge absorption spectra of phosphates. *Physica B*, **216**, 85-95

Giuli, G., Pratesi, G., Cipriani, C., Paris, E. (2003): Iron local structure in tektites and impact-glasses by EXAFS and high resolution XANES spectroscopy. *Geochim. Cosmochim. Acta*, in press.

Lazzarotto, A. & Liotta, D. (1991): Structural features of the lignitiferous basin of Santa Barbara, Upper Valdarno area. *Boll. Soc. Geol. It.*, **110**, 459-467.

Mandarino, J.A. (1981): The Gladstone-Dale relationship: Part IV. The compatibility concept and its application. *Canad. Mineral.*, **19**, 441-450.

McCammon, C.A. & Burns, R.G. (1980): The oxidation mechanism of vivianite as studied by Mössbauer spectroscopy. *Am. Mineral.*, **65**, 361-366.

Moore, P.B. (1971): The $Fe^{2+}{}_3(H_2O)_n(PO_4)_2$ homologous series: crystal-chemical relationships and oxidized equivalents. *Am. Mineral.*, **56**, 1-17.

Nickel, E.H. (1995): The definition of a mineral. *Can. Mineral.*, **33**, 689-690.

Nickel, E.H. & Grice, J.D. (1998): The IMA Commission on New Minerals and Mineral Names: Procedures and Guidelines on Mineral Nomenclature, 1998. *Can. Mineral.*, **36**, 913-926.

Piriou, B. & Poullen, J.F. (1987): Etude infrarouge des modes vibrationnels de l'eau dans la vivianite. *Bull. Minéral.*, **110**, 697-710.

Pollard, A.M., Thomas, R.G., Williams, P.A., Just, J., Bridge, P.J. (1991): The synthesis and composition of georgeite and its reactions to form other secondary copper (II) carbonates. *Mineral. Mag*, **55**, 163-166.

Popoff, P. (1906): Ueber zwei neue phosphorhaltige Mineralien von den Ufern der Strasse von Kertsch. *Centralblatt Mineral. Geol. Paläontol.*, **4**, 112.

Pratesi, G. (1993): Iron Phosphate Minerals from Santa Barbara mine (Tuscany). *Per. Mineral.*, **62**, 5-12.

Rodgers, K.A. (1986): Metavivianite and kerchenite: a review. *Mineral. Mag.*, **50**, 687-691.

Rogova, V.P., Belova, L.N., Kiziyarov, G.N., Koznetsova, N.N. (1974): Calciouranoite, a new hydroxide of uranium. *Zapiski Vses. Mineral. Obshch.*, **103**, 103-109 (in Russian).

Sagri, M. & Magi, M. (1992): Il bacino fluvio-lacustre del Valdarno Superiore. Field trip guide for the 76° Meeting of the Italian Geological Society, 201-226 (in Italian).

Spencer, L.J. (1925): Tenth list of new mineral names; with an index of authors. *Mineral. Mag.*, **20**, 448.

Waychunas, G.A., Apted, M.J., Brown, G.E. Jr. (1983): X-ray K-edge absorption spectra of Fe minerals and model compounds. *Phys. Chem. Minerals*, **10**, 1-9.

Wilke, M., Farges, F., Petit, P.E., Brown, G.E. Jr., Martin, F. (2001): Oxidation state and coordination of Fe in minerals: an Fe K XANES spectroscopic study. *Am. Mineral.*, **86**, 714-730.

Wong, J., George, G.N., Pickering, I.J., Reck, Z.U., Tanaka, T., Via, G.H., De Vries, B., Vaughan, D.E.W., Brown, G.E. Jr. (1994): New opportunity in XAFS investigation in the 1-2 KeV region. *Solid State Comm.*, **92**, 559-562.

*Received 3 April 2002*
*Modified version received 15 July 2002*
*Accepted 18 October 2002*